Structural and depositional controls on Plio-Pleistocene submarine channel geometry (Taranaki Basin, New Zealand)

Nathalia H. Mattos[1*], Tiago M. Alves[1] and Aisling Scully[2]

[1]3D Seismic Lab, School of Earth and Ocean Sciences, Cardiff University, Main Building-Park Place, CF10 3AT Cardiff, United Kingdom (mattosnh@cardiff.ac.uk)

[2]School of Biological, Earth and Environmental Sciences, University College Cork, Cork, Ireland

Abstract

High-quality 3D seismic data are used to investigate the effect of the Parihaka Fault on the geometry of submarine channels in Northern Graben of the Taranaki Basin, New Zealand. The Parihaka Fault comprises four segments (S1 to S4) with variable displacements. As part of the Plio-Pleistocene Giant Foresets Formation, the older Channel Complex Systems 1 and 2 reveal a two-stage evolution: 1) a syn-tectonic depositional stage with channels incising the slope during early fault growth (~4.5 Ma) and 2) a stage of sediment bypass (~3 Ma) leading to the infill of hanging-wall depocentres. Channel Complex System 3 is syn-tectonic relative to segment S3 and was formed at ~ 2.5 Ma. We show that the successive generation of new fault segments towards the north controlled the formation of depocentres in the study area. This occurred in association to rotation and uplift of the footwall block of the Parihaka Fault and subsidence of its hanging-wall block, with fault activity controlling the orientation of channel systems. As a result, we observe three drainage types in the study area: oblique, transverse and parallel to the Parihaka Fault. This work is important as it shows that relay zones separating the Parihaka Fault segments had limited influence on the geometry and location of channel systems. Submarine channels were diverted from their original courses close to the Parihaka Fault and flowed transversally to fault segments instead of running through relay ramps, contrasting to what is often recorded in the literature. A plausible explanation for such a discrepancy relates to rapid progradation of the Giant Foresets Formation during the Plio-Pleistocene, with channel complexes becoming less confined, favouring footwall incision and basinward deposition of submarine fans.

Keywords: New Zealand; Taranaki Basin; Parihaka Fault; relay ramps; submarine channels; stacking patterns.

1. Introduction

Relay ramps are a type of transfer zone developed between overlapping, reoriented fault segments that dip in the same direction (Fossen and Rotevatn, 2016; Gawthorpe and Hurst, 1993; Long and Imber, 2011; Peacock et al., 2000; Peacock and Sanderson, 1991). Relay ramps are formed either by the propagation and nucleation of initially isolated fault segments (the so-called isolated fault model) or following coherent fault models, in which the development of kinematically related segments result from the upward propagation of a reactivated fault (Childs et al., 2009; Giba et al., 2012).

Relay ramps are structures developed in rift basins that closely control the subaerial and subaqueous influx of sediment from footwall highs towards hanging-wall depocentres (Athmer et al., 2010; Athmer and Luthi, 2011; Fossen and Rotevatn, 2016; Gawthorpe and Hurst, 1993; Soreghan et al., 1999). Hence, the presence of relay ramps in tectonically active basins has a significant impact on sediment accommodation space, basin architecture and, consequently, on the deposition of reservoir units on hanging-wall depocentres (Athmer and Luthi, 2011; Gawthorpe and Hurst, 1993; Gupta et al., 1999; Ravnås and Steel, 1998). Relay ramps can change the course of fluvial systems by either obstructing their downslope flow or guiding sediment influx into alternative paths (Gee et al., 2007; Hopkins and Dawers, 2018). Previous studies have integrated observations of relay ramps from submarine settings with data from their subaerial (fluvial) to coastal analogues (Anderson et al., 2000; Athmer and Luthi, 2011; Mulrooney et al. 2018) to show the influence of faulting on the creation of accommodation space. However, the structural controls on accommodation and syn-rift deposition were only recently assessed in a submarine setting (Ge et al., 2017; Ge et al., 2018). This work aims at addressing the role of relay ramps as pathways for turbidity currents in an area with high-quality 3D seismic data.

In the Northern Graben of the Taranaki Basin, offshore New Zealand (Figs. 1a and 1b), a set of relay ramps was formed in the Late Cenozoic between four isolated fault segments of the Parihaka Fault (S1 to S4), with lengths varying from 8 km to 15 km (Giba et al., 2012). The Parihaka Fault is by itself part of the larger Cape Egmont Fault Zone and records: a) normal and left-lateral oblique reactivation during the Late Cretaceous, b) reverse displacement associated with the onset of andesitic volcanism in the Mid-Miocene, and c) oblique-slip movement during Plio-Pleistocene back-arc extension, which culminated in the opening of the Northern Graben (Giba et al., 2010; Hansen and Kamp, 2004a; King, 2000; King and Thrasher, 1996, Nodder, 1993) (Figs. 2a and 2b). High sedimentation rates accompanied the reactivation of the Parihaka Fault in the Plio-Pleistocene and led to the deposition of the Giant Foresets Formation, a thick syn-rift sequence comprising clinoforms incised by Pleistocene submarine channels (King and Thrasher, 1996; Salazar et al., 2016) (Fig. 2c).

This study investigates the control relay ramps exerted on the deposition of Late Pliocene strata in the Northern Graben, where laterally and vertically stacked submarine channels are identified within the Giant Foresets Formation (Fig. 2c). The identification of different drainage types in the Parihaka 3D seismic volume is complemented with the interpretation of channel geometries, reservoir prediction within channelised units, and by addressing the influence of the relay ramps on depositional systems in the Taranaki Basin. The relationship between different drainage types and regional faulting, as established in this work, will contribute to a more complete understanding of how fault systems control submarine channel geometries.

2. Geological Setting

The Taranaki Basin is a Cretaceous-Holocene asymmetric basin located to the west of New Zealand over an area of ~100.000 km^2 (King and Thrasher, 1996). The Taranaki Fault bounds the Taranaki Basin to the east

(Holt and Stern, 1991) (Fig. 1a). The western and southern limits of the Taranaki Basin are, respectively, the Challenger Plateau and the sub-basins of the South Island (Fig. 1a). To the northwest of the study area, the Taranaki Basin terminates in the New Caledonian Basin (King and Thrasher, 1996).

The Cape Egmont Fault Zone divides the Taranaki Basin into the relatively undeformed Western Stable Platform and the tectonically active Eastern Mobile Belt (King and Thrasher, 1996; Nodder, 1993) (Fig. 1b). The Eastern Mobile Belt comprises a Northern Graben, a Central Graben, and the buried Miocene Mohakatino Volcanic Centre (Hansen and Kamp, 2004a; Neall et al., 1986; Stagpoole and Funnell, 2001). The complex deformation history of the Eastern Mobile Belt includes extensional episodes that were concomitant with basin subsidence, and compression between the Australian and Pacific plates occurring from Late Cretaceous to Early Eocene (Giba et al., 2010; Holt and Stern, 1991; Holt and Stern, 1994; King and Thrasher, 1996; Nicol et al., 2005; Stagpoole and Nicol, 2008).

Oligocene subsidence chiefly affected the eastern part of the Taranaki Basin. During the earliest Miocene, basin subsidence gave way to compression resulting from westward thrusting along the Taranaki Fault (Kamp et al., 2004a; Kamp et al., 2004b; King, 2000; King and Thrasher, 1996; Nicol et al., 2004). Andesitic volcanic complexes were active in the Taranaki Basin from ~ 12 Ma to 6 - 4.8 Ma, resulting in the formation of the Mohakatino Volcanic Centre (Hansen and Kamp, 2004a). A high degree of uncertainty for the ages of volcanism in the Taranaki Basin results from the absence of continuously cored boreholes; these would allow the identification of stratal relations between volcanic and sedimentary units (Hansen and Kamp, 2004a).

Shortening in the south and extension in the north of the Taranaki Basin occurred concomitantly from the Miocene to the Plio-Pleistocene (Giba et al., 2010; Holt and Stern, 1994; Stagpoole and Nicol, 2008). Back-arc extension during the Early Pliocene led to the formation of the Northern Graben, an NNE-SSW fan-shaped graben delimited by the Cape Egmont Fault Zone to the west and by the Turi Fault Zone to the east (Giba et al., 2010; King, 2000; King and Thrasher, 1996) (Fig. 1b).

The Cape Egmont Fault Zone extends for more than 200 km along the western portion of the Taranaki Basin, comprising normal, reverse and *en echelon* faults (King and Thrasher, 1996; Nodder, 1993). The Parihaka Fault is one of the main structures of the Cape Egmont Fault Zone, consisting of four individual fault segments (S1 to S4 from south to north, Fig. 2a) that are 8 km to 15 km long, for a total length of approximately 50 km (Giba et al., 2012) (Figs. 1b and 2a). The southern segments of the Cape Egmont Fault Zone (S1 and S2) are hard-linked at Late Cretaceous level (Figs. 2b and 2c). Early Pliocene (3.7 Ma) back-arc extension reactivated segments S1 and S2 with a maximum vertical displacement of 600 m and, at the same time, formed the NE-striking segments to the north of the Cape Egmont Fault Zone (S3 and S4, Fig. 1b).

The reactivation of segments S1 and S2 ceased during the Pleistocene, whilst segments S3 and S4 continued to propagate in the Holocene, resulting in vertical displacements of up to 1450 m for segment S4 (Giba et al., 2012). Relay ramps were developed between segments S3 and S4 according to the coherent fault growth model of Walsh et al. (2003) (Fig. 2a). Thus, variations in fault strikes resulted in important rotation of the fault surface, producing a three-dimensional sigmoidal shape in cross-section (Fig. 2c). The growth of the Parihaka Fault along segments S3 and S4 was accommodated by later displacement and rotation of relay zones (Giba et al., 2012).

The Miocene – Quaternary stratigraphy of the Taranaki Basin is shown in detail in Figure 3. Miocene units are associated with the regressive Wai-ti Group and volcaniclastic sediments from the Mohakatino Formation (King and Thrasher, 1996). In the Northern Graben, the Plio-Pleistocene Rotokare Group includes prograding fan deposits of the basal Mangaa Formation, plus shelf and slope sediments of the Giant Foresets Formation (Hansen and Kamp, 2002). The studied interval is part of the Giant Foresets Formation, a ~2000 m-thick unit comprising fine sands and muds, characterised on seismic data by the presence of clinoforms and incised submarine channels (Hansen and Kamp, 2002, King and Thrasher, 1996; Salazar et al., 2016). High sedimentation rates recorded within the Giant Foresets Formation were responsible for preserving the growth history of the Parihaka Fault segment during the Plio-Pleistocene (King and Thrasher, 1996).

3. Data and Methods

3.1. Dataset

The Parihaka 3D volume covers a total area of 1,520 km^2 of the Taranaki Basin, at a maximum water depth of 150 m (Fig. 1b). The study area corresponds to a polygon with 705 km^2 around the Parihaka Fault segments (Fig. 2a). The zero-phased seismic dataset was acquired with an 8 x 4500 m array of streamers and later resampled at 4 ms TWT intervals. High-resolution Radon Transform linear noise attenuation, TAU-P domain deconvolution, and NMO corrections to the 60-fold coverage of the seismic trace preceded the processing of the seismic volume. A Kirchhoff time migration algorithm was then applied to 1 km grids. The final output is a stacked data volume with 12.5 x 12.5 m bins. Interpreted seismic profiles are displayed in normal SEG convention, with amplitude peaks shown in red and amplitude troughs in blue (see inset on Fig. 2c).

Well Arawa-1 was plugged and abandoned in the centre of the Parihaka 3D volume, and reached total depth of 3055 m (Arco, 1992). A dominant frequency of 40 Hz and an average velocity of 2000 m/s for the Plio-Pleistocene interval (Giba et al., 2012; Salazar et al., 2016) correspond to a vertical resolution of 12.5 m.

3.2. Channel interpretation methods

Seismic interpretation included fault and horizon mapping in Schlumberger's Petrel®. Interpreted horizons were numbered in chronological order from oldest to youngest, prefixed by the letter H (e.g., H_1, H_2, H_3). Horizons at the base and top of the main channel section (within H_2 and H_3) were labelled BC and TC, respectively (Fig. 2c). Biostratigraphical markers of Crundwell et al. (2004) and Morgans (2006) were used to correlate the stratigraphic interval of interest, which corresponds to strata with ages ranging from 4.5 to 2.4 Ma (seismic units SU2 and SU5 in Salazar et al., 2016).

Time-structural and thickness maps for horizons BC and TC were also generated (Fig. 4). In this work, velocity data were used to depth-convert the TWT thickness maps. Individual channels and channel complex systems were identified on seismic profiles as isolated or stacked U- and V- shapped erosional features based on amplitude contrasts between the channel-fill and its surroundings (Deptuck et al., 2003; Posamentier and Kolla, 2003).

The bounding surfaces of four large-scale submarine channel complex systems (Channel Complex Systems 1-4) were mapped using the procedure described by Deptuck et al. (2003). This procedure consists in the identification of the lowermost continuous channel incision surface on seismic profiles. Channel complexes represent groups of discrete submarine channels, while channel complex systems represent confined groups of channel complexes (Mayall et al., 2006). Submarine channels' hierarchical frameworks were thus identified based on: a) the geometry of channel fill strata, b) vertical and lateral channel stacking patterns, and c) the relative distribution of their bounding surfaces (Abreu et al., 2003; Clark and Pickering, 1996; Mayall et al., 2006). In addition, confined channels tend to exhibit important vertical stacking, whereas sinuous and less confined channels tend to show lateral stacking (Abreu et al., 2003; Clark and Pickering, 1996). Distinct stacking patterns in submarine channels result from gradual to abrupt shifts in their position(s).

The Parihaka 3D seismic volume was flattened to remove discontinuities and reveal periods of syn-depositional fault growth, thus highlighting the relationship between submarine channels and the Parihaka Fault (*cf.* Lee, 2001; Lomask, 2003). Faults bounding the relay ramps were identified on the seismic lines as overlapping, laterally continuous structures (Long and Imber, 2011) (Fig. 2c). We used horizon TC, with an estimated age of 2.45 Ma based on foraminifera samples (Salazar et al., 2016), as the reference horizon to flatten the seismic volume.

Horizon TC post-dates the onset of reactivation of the Parihaka Fault during the Plio-Pleistocene, allowing us to investigate the influence of this structure on Channel System Complexes 1 and 2. In order to include Channel System 3 in this analysis, we flattened the seismic cube using the top prograding horizon H_3 (1.26 Ma) as reference, as this channel system incises horizon TC (Fig. 2c).

The three-dimensional geometry of channels at depth was investigated using a quantitative approach. The distribution of channel system complexes was measured in relation to channel points (CP) located at the base of the channels (Gamboa et al., 2012) (Fig. 5a). The channel points (CP) method is scale- and survey-independent, consisting in the plotting of CPs at the base of channels on variance time slices. The maximum channel width between each sides of the channel complex system, and the maximum channel height measured from the top to the base of the channel complex system, were computed for each channel point. We used a spacing of 25 ms TWT between each time slice, at a depth varying between 864 ms and 2616 ms TWT. These depths correspond to the shallowest and the deepest submarine channels on the variance slices (Figs. 5b – 5e). The location of the channel points (X, Y, and Z) were exported into ArcMap and gridded using the ordinary kriging method with a polygon delimiting the study area. A channel point density map based on the overall spatial arrangement of the CPs was thus created to highlight the degree of variability in channel clustering and distribution.

4. Geometry of the main channel sequence and interaction with the Parihaka Fault segments

The interval of interest to this work is bounded at its base and top by horizons BC and TC (Figs. 2c and 4a). It is part of the Giant Foresets Formation (Fig. 3). Horizon BC is a medium- to high-amplitude positive reflection, continuous on the footwall of the Parihaka Fault, and offset by faults on its hanging-wall (Figs. 2c and 4a). The depth of Horizon BC ranges between 1250 ms and 1500 ms TWT on the footwall block, and between 2150 ms and 2250 ms TWT on the hanging-wall block, with an overall dip to the E and NE, respectively (Fig. 4a). Horizon BC correlates with the base of seismic unit SU2 in Salazar et al. (2016), dated as 4.5 Ma using foraminifera (Morgans, 2006).

Horizon TC is a medium- to high-amplitude positive reflection incised by small-scale channel tributaries and is offset by the Parihaka Fault (Figs. 2c and 4b). The base of horizon TC ranges in depth between 900 ms and 1050 ms TWT on the footwall block, and 950 ms and 1450 ms TWT on the hanging-wall block (Fig 4b). It corresponds to the top of the seismic unit SU5 of Salazar et al. (2016), with an assigned age of ~ 2.45 Ma (Morgans, 2006). The thickness of the main channel sequence, between horizons BC and TC, varies from 350 m to 400 m on the footwall block (Fig. 4c). The thickness of this same interval reaches its lowest value (200 - 250 m) along the discrete Parihaka Fault segments. On the hanging-wall block, two thickness maxima are observed between horizons BC and TC (500 – 800 m). They are referred herein as depocentres 1 and 2 (Fig. 4c).

The interval between BC and TC comprises high-amplitude prograding reflections incised either by single channel complex sets with a large erosional base, or by multiple basal tributaries with widths up to 1 km. These tributaries converge to form a large channel complex system (Fig. 6). Channel fill deposits are low- to medium-amplitude, chaotic and discontinuous reflections (Fig. 6). Evidence for vertical and lateral stacking of the channel bodies is observed throughout the study area (Fig. 6). Four channel complex systems, named 1 to 4, were thus identified (Figs. 7 to 10).

4.1. Channel Complex System 1

Channel Complex System 1 is a ~27 km long conduit offset by segment S1 (Figs. 7a and 7b). This channel complex system extends beyond the limits of the seismic volume. The erosive base of the channel complex system is observed on seismic at a maximum depth of 1100 ms TWT below the sea floor. Isolated channels with widths up to 1 km and thicknesses of up to 200 m are recognised as tributaries to this channel system on the footwall block (Fig. 6a).

Segment S1 shows a horsetail geometry in the southern section (section A-B, Fig. 6a), comprising faults initiated below horizon BC that propagate to a depth of 1250 ms TWT. Lateral migration at the base of this channel complex system indicates a deflection of the channel course, and vertically stacked channel complex deposits are observed on the hanging-wall block (Fig. 6a).

The channel complex sets in the central profiles (profiles C-D and E-F; Figs. 6b and 6c) are characterised by planar to slightly concave-upward basal surfaces in a multistorey (nested) offset stacking arrangement. In section E-F, Channel Complex System 1 reaches its maximum width (10.4 km), as deposits seem to be less confined, a character suggesting the deposition of multiple submarine fans. In the northern section, the erosive base of Channel Complex System 1 is clearer than in section E-F, and multiple planar to slightly concave upward lobate surfaces are observed (section G-H; Fig. 6d). The main channel direction in the footwall block is SW-NE, with two main branches forming angles of 44° and 65° with respect to segment S1 (Fig. 7a). A third tributary is perpendicular to the trace of segment S1, whereas the northernmost tributary of Channel Complex System 1 forms an angle of 85° to this segment (Fig. 7a). This channel system is oblique in relation to S1. Channel Complex System 1 changes its sinuosity to the SE of the study area, where meandering channels are observed on the hanging-wall block (Figs. 7a and 7b).

Confluence of these branches occurs on the fault-bounded slope, and a single conduit is observed on the hanging-wall block ranging in with from 0.9 km to 3.3 km. Away from S1, this channel system reaches thicknesses of up to 350 metres (Fig. 7b), coinciding with the location of Depocentre 1 (Fig. 4c). In the unflattened seismic section a similar channel-fill reflection pattern, with continuity interrupted by S1, is observed on both the footwall and hanging-wall blocks (Fig. 7c). In the flattened seismic section, using horizon TC as a reference, the removal of segment S1 allows the reconstruction of the original position of Channel Complex System 1, suggesting that reactivation of S1 around 3.7 Ma generated accommodation space on its immediate hanging-wall block (Fig 7d).

4.2. Channel Complex System 2

Channel Complex System 2 is a ~15 km-long channel complex system located in the central part of the study area, within the limits of the Parihaka 3D volume (Fig. 8). The confined base of this channel complex system initially forms an angle of 61° to the NNE-striking segment S2 on the footwall block. It then forms a perpendicular angle to S2 on the hanging-wall block (Figs. 8a and 8b). This channel system is thus classified as being transverse to S2. Channel orientation downdip varies from SW-NE to W-E, adjacent to S2, to SW-NE towards the limits of the seismic survey (Fig. 8b).

Channel Complex System 2 shows similar sinuosity to Channel Complex System 1, i.e. it is sinuous on the footwall and meandering on the hanging-wall (Figs. 8a and 8b). When compared to Channel Complex System 1, its vertical stacking becomes less marked near the Parihaka Fault (Fig. 6c). On the hanging-wall, the channel complex system becomes less confined towards de NE (Fig. 8b) where a maximum thickness of 300 m is observed. Accommodation space was created during the reactivation of S2, as this fault segment is continuous on the seismic profiles flattened at horizon TC (Figs. 8c and 8d). The geometry of the relay ramp developed between segments S2 and S3 shows rotation of S2 in relation to the footwall and the hanging-wall blocks (Fig. 6c), with subsequent development of horsetail splays at its upper tip, offsetting Channel System 2.

4.3. Channel Complex System 3

Channel Complex System 3 is >15 km long and located in the northern part of the study area (Figs. 9a and 9b). The base of this channel complex system incises horizon TC close to segment S3 (Fig. 9a). It then migrates towards the NE, where it deepens to 1450 ms TWT (Fig. 9b). This channel system is characterised by two tributaries that form angles of 71^{o} and 60^{o} relative to the NNE-striking segment S3 (Fig. 9a).

Channel Complex System 3 is an example of a channel system transverse to S3 (Figs. 9a and 9b). Channel confluence occurs on the fault-bounded slope formed between the footwall and hanging-wall blocks, and Channel Complex System 3 becomes perpendicular to the Parihaka Fault towards the east, where it reaches its maximum thickness (300 m). In contrast to Channel Complex Systems 1 and 2, this channel system does not show a dramatic decrease in confinement close to depocentre 1.

A ~ 4 km width relay ramp comprising segments S2 and S3 of the Parihaka Fault is observed to the south of Channel Complex System 3 (see section E-F, Fig. 6c), whereas a ~ 500 m width relay ramp formed between segments S3 and S4 occurs to the north (see section G-H, Fig. 6d). Despite the occurrence of these two relay ramps, Channel Complex System 3 flows transversally to S3. Channel Complex System 3 is mostly sinuous, on both the footwall and hanging-wall blocks (Figs. 9a and 9b).

As Channel Complex System 3 incises horizon TC, and is thus younger than 2.5 Ma, we flattened the seismic profile in Fig. 9c using horizon H_3 (1.26 Ma) as reference. The flattening reveals a continuous S3, and suggests that the development and growth of this fault segment had an important role in the creation of accommodation space later filled by Channel Complex System 3 (Fig. 9d).

4.4. Channel Complex System 4

Channel Complex System 4 is a >18 km long meandering channel complex system located in the northern part of the study area. It incises a prograding sequence on the footwall block (Fig. 10a). This channel complex system is not offset by any of the Parihaka Fault segments. However, at a distance of 2 km from S3, the erosive base of the channel changes from SW to NW, following a direction that is initially parallel to S3 to then trends 53^{o} to NW.

Channel System 4 remains mostly confined and reaches a maximum thickness of 300 m towards the end of the seismic survey (Fig. 10b). This conduit was filled in a series of multistorey nested offset to vertically stacked channel complex sets, before changing its course to NW (Figs. 6c and 10c).

5. Channel density in the study area

Channel Point (CP) distribution maps (Fig. 5b to 5e), and corresponding density plots (Fig. 11), reveal that channels occur predominantly between 864 ms and 1152 ms TWT on the footwall block (Figs. 5b and 11). Channel Points for Channel Complex System 4 are concentrated in the interval between 1152 ms and 1440 ms TWT (Fig. 5c). A large channel is observed in the southwestern portion of the study area at a depth ranging from 1440 ms to 1728 ms TWT (Fig. 5d). Channel points on the hanging-wall block predominate at depths ranging from 1152 ms to 1440 ms TWT and 1440 ms to 1728 ms TWT (Figs. 5c and 5d). Only a small number of channels were recorded between 1728 ms and 2016 ms TWT (Fig. 5e).

Two areas of relatively high channel concentration are observed on density point data (Fig. 11). The first area corresponds to the position of Channel Complex System 4 on the footwall block. The second area is located adjacently to the hanging-wall of S2, in the position of Channel Complex System 2 (Fig. 11). Figure 11 also shows a medium channel density in the areas corresponding to Channels Systems 1 and 3. Channel density is low adjacently to the three relay ramps developed between the Parihaka Fault segments (Fig. 11).

6. Discussion

6.1. The Parihaka Fault and associated drainage systems

In this work, two factors emerge as major controls on the creation of hanging-wall depocentres: 1) the reactivation of the Parihaka Fault segments S1 and S2, and the later development of S3 and S4, and 2) the high sedimentation rates recorded in the Taranaki Basin during the Plio-Pleistocene. These two controls are interpreted to have influenced channel evolution and distribution at different scales (Fig. 12). In the study area, three main drainage types related to the orientation of fault segments are observed: oblique, transverse, and parallel drainage (Fig. 12). The distribution, position and thickness of each of these drainage types were controlled by the orientation of the fault segments, fault displacement and tectonic subsidence rates (Eliet and Gwathorpe, 1995; Ge et al., 2017; Henstra et al., 2016; Morgan, 2004; Ravnås and Steel, 1998; Soreghan et al., 1999).

Channel Complex System 1 is an example of an oblique drainage system where its largest tributary, located in the southern part of the study area, forms an angle of 44° relative to S1 (Figs. 7a and 12). Two other tributaries of this channel system, forming angles of 65° and 71° relative to segment S1, are also identified on the footwall block (Fig. 7b). On the hanging-wall block, multistorey vertically and laterally nested channel complex sets are observed (Fig. 7c).

The flattened seismic section in Fig. 7d suggests that Channel Complex System 1 was initially developed in the southern part of the study area, before S1 was reactivated in the Early Pliocene. However, from Fig. 12 one can also observe a clear relationship between the angles between tributaries in Channel Complex System 1 and segment S1. Fault throw is also larger towards the centre of the fault, where channel tributaries converge, indicating that the reactivation of segment S1 affected the channels (Fig. 12) by creating accommodation space on the hanging-wall block (Fig. 4c).

Channel Complex System 2 is an example of a transverse drainage system showing deflection of its initial path towards the trace of segments S2 and S3 (Fig. 8). Deflections in Channel Complex System 2 reveal that channel evolution was controlled by fault orientation and uplift and rotation of the footwall block (Hubbard et al., 2014; Soreghan et al., 1999). The seismic profile flattened on horizon TC shows a continuous segment S2 at 2.45 Ma, suggesting that it was active at this time and contributing to the creation of accommodation space on the hanging-wall block (Fig. 8d). It also indicates that downslope progradation of the Giant Foresets

Formation sediments, downstream of segments S1 and S2, occurred in at least two phases when considering Channel Complex Systems 1 and 2. The first phase (~4.5 Ma) is syn-tectonic and related to incision of the fault-bounded slope between the footwall and hanging-wall blocks, corresponding to the early stages of fault growth and subsidence of the Northern Graben (Giba et al., 2012). The second phase (~3 Ma) is related to a relative sea level lowstand and is characterised by sediment bypass towards the basin depocentre (Salazar et al., 2016). It deposited relatively less confined, thicker deposits (Figs. 8c and 8d).

Channel Complex System 3 is another example of a transverse drainage system. In contrast to Channel Complex System 2, this channel system incises horizon TC with two tributaries that converge on the slope of S3. Such a geometry indicates that the deposition of Channel Complex System 3 occurred during the Late Pliocene, whereas Channel Complex Systems 1 and 2 developed during the Early Pliocene. The geometry of Channel Complex System 3 highlights the active growth of segment S3 (Fig. 9).

Transverse channel migration was responsible for both lateral migration and vertical stacking of channels in the study area. The syn-tectonic evolution of Channel Complex Systems 2 and 3, due to reactivation of S2 and onset of S3 is characteristic of half-graben systems showing transverse drainage systems, and common in areas of active extensional tectonics (Ge et al., 2017; Ravnås and Steel, 1998). An analogue example is observed in the Niger Delta, where half-grabens have continuously controlled the position and distribution of turbidite channel complexes in proximal areas of the Nigeria's continental slope (Morgan, 2004).

Channel Complex System 4 is located on the footwall block of the Parihaka Fault, with an initial SW-NE direction (Figs. 10a and 10b). Instead of following oblique to transverse pathways in relation to the fault trace, Channel Complex System 4 is deflected in the proximity of S3. The movement of S3 and S4 in the northern part of the study area resulted in the rotation and uplift of the footwall block close to the fault scarp. This is the main cause for the diversion of Channel Complex System 4 to the NW of the study area (Figs. 10a and 10b).

Local subsidence along the Parihaka Fault is interpreted from the sediment thickness map extracted between horizons BC and TC, where two depocentres were developed on the hanging-wall block towards the NE (Fig. 4c). The generation of accommodation space in Depocentres 1 and 2, and the large volume of sediment accumulated on the hanging-wall block, indicate the Parihaka Fault controlled the distribution of sediments in the study area. Relative isolation of the footwall block and marked thickening of strata on the hanging-wall block are particularly observed along the Early Pliocene - Recent segments S3 and S4.

The sinuosity values observed for Channel Complex Systems 1 to 3 indicate that channels are more sinuous on the footwall block. On the hanging-wall block, channels vary from straight to meandering and show a complex geometry, with complex vertical and lateral stacking patterns in channel complex sets. Changes in the dip directions of channel incisions due to an increase in the slope (Deptuck et al., 2003; Gee and Gawthorpe, 2006) are also observed. This occurs due to the levelling out of the hanging-wall slope as strata thickens (Gawthorpe and Leeder, 2000), favouring progradation in areas of high sediment supply.

6.2. Limited influence of relay ramps on sediment sourcing into hanging-wall deposition

Displacement accommodation between individual fault segments is often enhanced by the formation of intrabasin transfer zones or relay ramps, especially when the geometry of faults follows an en echelon stepping pattern (Leeder and Gawthorpe, 1987). Intrabasin relay ramps may influence sedimentation trends on a local scale to act as pathways for turbidity currents, especially in transverse drainage systems (Anderson et al., 2000; Athmer et al., 2010; Fugelli and Olsen, 2007; Gawthorpe and Hurst, 1993; Ravnås and Steel, 1998; Rotevatn et al., 2007; Young et al., 2001). A decrease in elevation towards the ramp is normally associated with intrabasin transfer zones (Gawthorpe and Hurst, 1993; Paul and Mitra, 2013). Individual transfer zone morphologies, however, are poorly constrained on subsurface data (Gawthorpe and Hurst, 1993; Gibbs, 1989).

The relay ramps developed between the Parihaka Fault segments are well-preserved in our seismic volume. Giba et al. (2012) examined the kinematic evolution of the relay zone developed between segments S1 and S2, which shows an overlap of 2.8 km. The transfer zone developed between segments S2 and S3 of the Parihaka Fault is fully breached and could act as a conduit for sediment flow onto the hanging wall. One could expect Channel Complex System 3 to follow this relay ramp. However, Channel Complex System flows transversally to S3 instead of flowing towards the relay ramp, forming a more abrupt sediment pathway towards the hanging-wall block. This likely occurred due to the effectiveness of the channel systems in containing sediment flow while incising the slope.

The geometry of relay ramps in the study area is consistent with the axial through-drainage facies model of Leeder and Gawthorpe (1987), in which mini-grabens developed in the zone between two *en echelon* normal faults confine the channel deposits as vertically-stacked units bounded by faults. However, the transverse orientation of the channels flowing towards the Parihaka Fault segments, the absence of interpreted submarine fans on the seismic profiles, and cross-correlations between channel-density (Fig. 11) and thickness data (Fig. 4c), do not show a concentration of channels around the transfer zones to support the trapping of channel deposits by relay ramps.

A ~ 500 m width transfer zone developed between segments S3 and S4 was identified as an unbreached relay ramp, as these segments are not linked at depth (Fig. 6d). Its development resulted from the large displacement of the northern section of the fault system due to its sub-optimal strike in relation to regional extension. The large displacement recorded in the northern part of the study area led to repeated rotation of beds in the relay ramp, and significant hanging-wall deformation (Giba et al., 2012), a factor accounting for the lower gradient slope and offset in this zone. The submarine channels surrounding the ramp do not show a clear convergence of footwall drainage systems flowing through the relay ramp, preferentially feeding into the hanging wall sub-basin.

6.3. Channel deposit thickness and implications for petroleum systems

While significant subsidence occurred in the Taranaki Basin during the Cretaceous-Eocene (Giba et al., 2012; King and Thrasher, 1996), this study focuses on the Pliocene syn-rift phase, in which submarine channel complex systems were able to form. The thickness map of the main channel section (between horizons BC and TC; Fig. 4c) and seismic profiles in Figs. 7 to 10 indicate that the accommodation space was primarily located on the hanging-wall block of the Parihaka Fault system, where two depocentres were formed to the NE of the study area (Fig. 4c). However, the great thickness of the hanging-wall block is not reflected in the channel density plot (Fig. 11), where channel density is shown to be larger around Channel Complex Systems 2 and 4. Evidence for channels close to relay ramps is scarce both on the channel density plot (Fig. 11) and on the isochron map in Fig. 4c. This latter observation proves the minor influence that relay ramps had on channel configuration (Fig. 11).

Fault activity in the Cape Egmont Fault Zone may have an important control on petroleum system in the North Taranaki Graben. The deposition of the Giant Foresets Formation during the Pliocene was synchronous with the growth of the Parihaka Fault and subsequent generation of accommodation space on the hanging-wall block, resulting in the formation of two depocentres in the NE. Vertically and laterally stacked channel deposits of Channel Complex Systems 2 and 3, on the hanging-wall of the Parihaka Fault, comprise a potential reservoir for hydrocarbons generated in the Moki Formation. As thick channel deposits are observed on the hanging-wall block, they will be important for the development of petroleum systems in the northern Taranaki Basin (Armstrong et al., 1996; Funnell et al., 1996; Hansen and Kamp, 2004b; Webster et al., 2011).

The rapid deposition of sediment in the Giant Foresets Formation can either influence the migration of hydrocarbons or comprise a potential hydrocarbon reservoir seal (Stagpoole and Funnell, 2001). Rapid sediment accumulation rates during basin development may also contribute to increasing thermal gradients, hydrocarbon maturation and migration through a petroleum system (Spencer, 1987). However, no evidence for fluid accumulations were found in the interpreted seismic data. The well Arawa-1 recorded three significant dry gas peaks at the top of the Moki Formation, below the interval of interest of this work (Arco, 1992). Based on the interactions between tectonic subsidence and fast sedimentation related to the opening of the Northern Graben we can infer any fluids generated in the study area migrated upwards along the Parihaka Fault.

7. Conclusions

The importance of structural controls on submarine channel deposits motivated the analysis of the Parihaka 3D seismic volume as a case study that can be extrapolated to other areas where faulting influences the geometry of channel drainage networks. In parallel, this study aimed at evaluating the location of large depocentres on the hanging-wall block of the Parihaka Fault, some with potential reservoir intervals. The main conclusions of this work can be summarised as follows:

a) The reactivation of segments S1 and S2 in the Parihaka Fault (Early Pliocene to Pleistocene) and the formation of segments S3 and S4 from 2.4 Ma until the present day, generated important accommodation space. This is demonstrated by the formation of two large depocentres on the hanging-wall block of the Parihaka Fault.

b) Transverse, oblique and parallel drainage types were developed relative to the Parihaka Fault. Channel Complex System 1, located in the southern part of the study area, is an example of a drainage system flowing obliquely to S1 during the reactivation of this segment. Channel Complex Systems 2 and 3 initially flow obliquely to the Parihaka Fault and are later diverted transversally, incising segments S2 and S3. Channel Complex System 4 flows parallel to the fault trace on the footwall block due to footwall uplift associated with segments S3 and S4.

c) Relay Ramps were developed between distinct fault segments. However, submarine channels did not use the relay ramps as main pathways for the sediments. Channel Complex Systems 2 and 3, for instance, changed their original courses and flowed transversally relative to the Parihaka Fault trace, instead of flowing through the relay ramps.

d) Channel systems are concentrated on both the footwall and hanging-wall blocks of the Northern Graben, with two depocentres identified in the NE. We propose that Channel Complex System 2, on the footwall block, comprises an important hydrocarbon reservoir in the study area. Vertically- and laterally-stacked channel complex systems, where the progradational sequences of the Giant Foresets Formation rapidly accumulated on the hanging-wall block, may also comprise competent reservoir units in the study area.

Acknowledgments

The authors would like to acknowledge the New Zealand Petroleum Board for the use of data included in this paper. The first author would like to acknowledge CAPES (Coordenação de Aperfeiçoamento de Pessoal de Nível Superior – Brazil) for the PhD grant no. 99999.000877/2014-00. Schlumberger is acknowledged for the provision of the academic licences of Petrel® to Cardiff University 3D Seismic Lab. We thank Editor Atle Rotevatn, Migdalys Salazar, Larissa Hansen and Clark Gilbert for their constructive comments on this manuscript.

References

Abreu, V., Sullivan, M., Pirmez, C., & Mohrig, D. 2003. Lateral accretion packages (LAPs): an important reservoir element in deep water sinuous channels. *Marine and Petroleum Geology*, 20(6-8), 631-648.

Anderson, J.E., Cartwright, J., Drysdall, S.J., Vivian, N., 2000. Controls on turbidite sand deposition during gravity-driven extension of a passive margin: examples from Miocene sediments in Block 4, Angola. *Marine and Petroleum Geology*, 17, 1165-1203.

Arco Petroleum, 1992. Arawa-1 Final Well Report PPL 38436, in Ministry of Economic Development, New Zealand: Crown Minerals Unpublished Petroleum Report, PR 1824.

Armstrong, P.A., Chapman, D.S., Funnell, R.H., Allis, R.G., Kamp, P.J., 1996. Thermal modeling and hydrocarbon generation in an active-margin basin: Taranaki Basin, New Zealand. *AAPG Bulletin* 80, 1216-1241.

Athmer, W., Groenenberg, R.M., Luthi, S.M., Donselaar, M.E., Sokoutis, D., & Willingshofer, E. 2010. Relay ramps as pathways for turbidity currents: a study combining analogue sandbox experiments and numerical flow simulations. *Sedimentology*, 57(3), 806-823.

Athmer, W., Luthi, S.M., 2011. The effect of relay ramps on sediment routes and deposition: A review. *Sedimentary Geology* 242, 1-17.

Childs, C., Manzocchi, T., Walsh, J. J., Bonson, C. G., Nicol, A., & Schöpfer, M. P. 2009. A geometric model of fault zone and fault rock thickness variations. *Journal of Structural Geology*, 31(2), 117-127.

Clark, J. D., & Pickering, K. T. 1996. Architectural elements and growth patterns of submarine channels: application to hydrocarbon exploration. *AAPG Bulletin*, 80(2), 194-220.

Crundwell, M.P.; Beu, A.G.; Morgans, H.E.G.; Mildenhall, D.C.; Wilson, G.S. 2004: Chapter 12, Miocene. In Cooper, R.A. (ed.) 2004. The New Zealand Geological Timescale. Institute of Geological and Nuclear Sciences Monograph 22. 284 p.

Deptuck, M. E., Steffens, G. S., Barton, M., & Pirmez, C. 2003. Architecture and evolution of upper fan channel-belts on the Nger Delta slope and in the Arabian Sea. *Marine and Petroleum Geology*, 20(6), 649-676.

Eliet, P. P., & Gawthorpe, R. L. 1995. Drainage development and sediment supply within rifts, examples from the Sperchios basin, central Greece. *Journal of the Geological Society*, 152(5), 883-893.

Fossen, H., & Rotevatn, A. 2016. Fault linkage and relay structures in extensional settings—A review. *Earth-Science Reviews*, 154, 14-28.

Fugelli, E.M., Olsen, T.R. 2007. Delineating confined slope turbidite systems offshore mid-Norway: The Cretaceous deep-marine Lysing Formation. *AAPG Bulletin*, 91(11), 1577-1601.

Funnell, R., Chapman, D., Allis, R., Armstrong, P., 1996. Thermal state of the Taranaki basin, New Zealand. *Journal of Geophysical Research: Solid Earth* (1978–2012) 101, 25197-25215.

Gamboa, D., Alves, T.M., Cartwright, J., 2012. A submarine channel confluence classification for topographically confined slopes. *Marine and Petroleum Geology*, 35, 176-189.

Gawthorpe, R.L., Fraser, A.J., Collier, R.E.L. 1994. Sequence stratigraphy in active extensional basins: implications for the interpretation of ancient basin-fills. *Marine and Petroleum Geology*, 11(6), 642-658.

Gawthorpe, R.L., Hurst, J., 1993. Transfer zones in extensional basins: their structural style and influence on drainage development and stratigraphy. *Journal of the Geological Society,* 150, 1137-1152.

Gawthorpe, R.L., Leeder, M.R. 2000. Tectono-sedimentary evolution of active extensional basins. *Basin Research*, 12(3-4), 195-218.

Ge, Z., Nemec, W., Gawthorpe, R. L., & Hansen, E. W. 2017. Response of unconfined turbidity current to normal-fault topography. *Sedimentology*, 64(4), 932-959.

Ge, Z., Nemec, W., Gawthorpe, R. L., Rotevatn, A., & Hansen, E. W. 2018. Response of unconfined turbidity current to relay-ramp topography: insights from process-based numerical modelling. *Basin Research*, 30(2), 321-343.

Gee, M., Gawthorpe, R., 2006. Submarine channels controlled by salt tectonics: Examples from 3D seismic data offshore Angola. *Marine and Petroleum Geology* 23, 443-458.

Gee, M., Gawthorpe, R., Bakke, K., Friedmann, S., 2007. Seismic geomorphology and evolution of submarine channels from the Angolan continental margin. *Journal of Sedimentary Research* 77, 433-446.

Giba, M., Nicol, A., Walsh, J., 2010. Evolution of faulting and volcanism in a back-arc basin and its implications for subduction processes. *Tectonics* 29.

Giba, M., Walsh, J.J., Nicol, A., 2012. Segmentation and growth of an obliquely reactivated normal fault. *Journal of Structural Geology* 39, 253-267.

Gibbs, A.D. 1989. Structural styles in basin formation. In: Extensional Tectonics and Stratigraphy of the North Atlantic Margins. *AAPG Memoir*. Vol. 46, pp. 81-94.

Gupta, S., Underhill, J., Sharp, I., Gawthorpe, R., 1999. Role of fault interactions in controlling synrift sediment dispersal patterns: Miocene, Abu Alaqa Group, Suez Rift, Sinai, Egypt. *Basin Research* 11, 167-189.

Hansen, R.J., Kamp, P.J., 2002. Evolution of the Giant Foresets Formation, northern Taranaki Basin, New Zealand.

Hansen, R.J., Kamp, P.J., 2004a. Late Miocene to early Pliocene stratigraphic record in northern Taranaki Basin: condensed sedimentation ahead of Northern Graben extension and progradation of the modern continental margin. *New Zealand journal of geology and geophysics* 47, 645-662.

Hansen, R.J., Kamp, P.J., 2004b. Rapid progradation of the Pliocene-Pleistocene continental margin, northern Taranaki Basin, New Zealand, and implications, Proceedings of New Zealand Petroleum Conference, pp. 7-10.

Henstra, G. A., Gawthorpe, R. L., Helland-Hansen, W., Ravnås, R., & Rotevatn, A. 2016. Depositional systems in multiphase rifts: seismic case study from the Lofoten margin, Norway. *Basin Research*. doi: 10.1111/bre.12183

Holt, W., Stern, T., 1991. Sediment loading on the western platform of the New Zealand continent: Implications for the strength of a continental margin. *Earth and planetary science letters* 107, 523-538.

Holt, W., Stern, T., 1994. Subduction, platform subsidence, and foreland thrust loading: The late Tertiary development of Taranaki Basin, New Zealand. *Tectonics* 13, 1068-1092.

Hopkins, M.C., Dawers, N.H. 2018. The role of fault length, overlap and spacing in controlling extensional relay ramp fluvial system geometry. *Basin Research*, 30(1), 20-34.

Hubbard, S.M., Covault, J.A., Fildani, A. and Romans, B.W., 2014. Sediment transfer and deposition in slope channels: deciphering the record of enigmatic deep-sea processes from outcrop. Bulletin, vol. 126, no. 5-6, pp.857-871.

Kamp, P.J., Vonk, A.J., Bland, K.J., Hansen, R.J., Hendy, A.J., McIntyre, A.P., Ngatai, M., Cartwright, S.J., Hayton, S., Nelson, C.S., 2004a. Neogene stratigraphic architecture and tectonic evolution of Wanganui, King Country, and eastern Taranaki Basins, New Zealand. *New Zealand Journal of Geology and Geophysics* 47, 625-644.

Kamp, P.J., Vonk, A.J., Nelson, C.S., Hansen, R.J., Tripathi, A.R.P., Hood, S.D., Nagati, M., Hendy, A.J., 2004b. Constraints on the evolution of Taranaki Fault from thermochronology and basin analysis: Implications for the Taranaki Fault play.

King, P.R., 2000. Tectonic reconstructions of New Zealand: 40 Ma to the present. *New Zealand Journal of Geology and Geophysics* 43, 611-638.

King, P.R., Thrasher, G.P., 1996. Cretaceous Cenozoic geology and petroleum systems of the Taranaki Basin, New Zealand. Institute of Geological & Nuclear Sciences.

Lee, R. F. 2001. Pitfalls in seismic data flattening. *The Leading Edge*, 20(2), 160-164.

Leeder, M., Gawthorpe, R., 1987. Sedimentary models for extensional tilt-block/half-graben basins. *Geological Society, London, Special Publications* 28, 139-152.

Lomask, J. 2003. Flattening 3-D data cubes in complex geology. Stanford Exploration Project, Report, 113, 247-261.

Long, J. J., Imber, J. 2011. Geological controls on fault relay zone scaling. *Journal of Structural Geology*, 33(12), 1790-1800.

Mayall, M., Jones, E., & Casey, M. 2006. Turbidite channel reservoirs—Key elements in facies prediction and effective development. *Marine and Petroleum Geology*, 23(8), 821-841.

Morgan, R. (2004). Structural controls on the positioning of submarine channels on the lower slopes of the Niger Delta. *Geological Society, London, Memoirs*, 29(1), 45-52.

Morgans, H. E. G. 2006. Foraminiferal Biostratigraphy of the Early Miocene to Pleistocene Sequences in Witiora-1, Taimana-1, Arawa-1 and Okoki-1. GNS Science.

Mulrooney, M. J., Rismyhr, B., Yenwongfai, H. D., Leutscher, J., Olaussen, S., & Braathen, A. 2018. Impacts of small-scale faults on continental to coastal plain deposition: Evidence from the Realgrunnen Subgroup in the Goliat field, southwest Barents Sea, Norway. *Marine and Petroleum Geology*, 95, 276-302.

Neall, V., Stewart, R., Smith, I., 1986. History and petrology of the Taranaki volcanoes. *Royal Society of New Zealand Bulletin* 23, 251-263.

Nicol, A., Stagpoole, V., Maslen, G., 2004. Structure and petroleum potential of the Taranaki fault play, New Zealand Petroleum Conference Proceedings, pp. 7-10.

Nicol, A., Walsh, J., Berryman, K., Nodder, S., 2005. Growth of a normal fault by the accumulation of slip over millions of years. *Journal of Structural Geology* 27, 327-342.

Nodder, S.D., 1993. Neotectonics of the offshore Cape Egmont Fault Zone, Taranaki Basin, New Zealand. *New Zealand journal of geology and geophysics* 36, 167-184.

Paul, D., Mitra, S. 2013. Experimental models of transfer zones in rift systems. *AAPG bulletin*, 97(5), 759-780.

Peacock, D. C. P., Knipe, R. J., & Sanderson, D. J. 2000. Glossary of normal faults. *Journal of Structural Geology*, 22(3), 291-305.

Peacock, D. C. P., & Sanderson, D. J. 1991. Displacements, segment linkage and relay ramps in normal fault zones. *Journal of Structural Geology*, 13(6), 721-733.

Pindell, J.L., 1995. Circum-Caribbean sedimentary basin development and timing of hydrocarbon maturation as a function of Caribbean plate tectonic evolution.

Posamentier, H. W., & Kolla, V. 2003. Seismic geomorphology and stratigraphy of depositional elements in deep-water settings. *Journal of sedimentary research*, 73(3), 367-388.

Ravnås, R., & Steel, R. J. 1998. Architecture of marine rift-basin successions. *AAPG Bulletin*, 82(8), 1626-1626.

Rotevatn, A., Fossen, H., Hesthammer, J., Aas, T.E., Howell, J.A. 2007. Are relay ramps conduits for fluid flow? Structural analysis of a relay ramp in Arches National Park, Utah. *Geological Society, London, Special Publications*, 270(1), 55-71.

Salazar, M., Moscardelli, L., Wood, L., 2016. Utilising clinoform architecture to understand the drivers of basin margin evolution: a case study in the Taranaki Basin, New Zealand. *Basin Research* 28, 840-865.

Soreghan, M. J., Scholz, C. A., & Wells, J. T. 1999. Coarse-grained, deep-water sedimentation along a border fault margin of Lake Malawi, Africa; seismic stratigraphic analysis. *Journal of Sedimentary Research*, 69(4), 832-846.

Spencer, C.W., 1987. Hydrocarbon generation as a mechanism for overpressuring in Rocky Mountain region. *AAPG Bulletin* 71, 368-388.

Stagpoole, V., Funnell, R., 2001. Arc magmatism and hydrocarbon generation in the northern Taranaki Basin, New Zealand. *Petroleum Geoscience* 7, 255-267.

Stagpoole, V., Nicol, A., 2008. Regional structure and kinematic history of a large subduction back thrust: Taranaki Fault, New Zealand. *Journal of Geophysical Research: Solid Earth* 113, n/a-n/a.

Walsh, J., Bailey, W., Childs, C., Nicol, A., Bonson, C., 2003. Formation of segmented normal faults: a 3-D perspective. *Journal of Structural Geology* 25, 1251-1262.

Webster, M., O'Connor, S., Pindar, B., Swarbrick, R., 2011. Overpressures in the Taranaki Basin: Distribution, causes, and implications for exploration. *AAPG Bulletin* 95, 339-370.

Young, M.J., Gawthorpe, R.L., Hardy, S. 2001. Growth and linkage of a segmented normal fault zone; the Late Jurassic Murchison–Statfjord North Fault, northern North Sea. *Journal of Structural Geology*, 23(12), 1933-195.

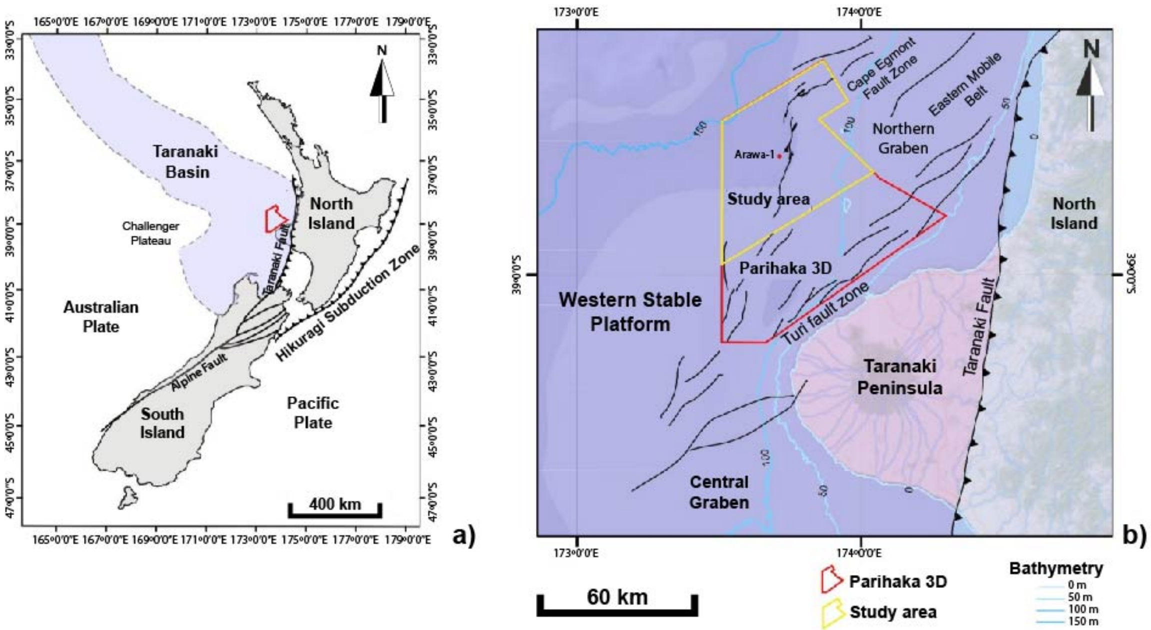

Figure 1: a) Regional location map of New Zealand and its main structural boundaries. The Taranaki Basin is limited to the east by the Taranaki Fault and to the west by the Challenger Plateau. To the south, the Taranaki Basin is limited by the South Island. The 3D seismic cube is delimited by the red polygon. b) Detailed location map of the Northern Graben showing the main structures at a local scale. The study area occurs between 100 and 150 m below the sea level. The 705 km^2 study area is delimited by the yellow polygon.

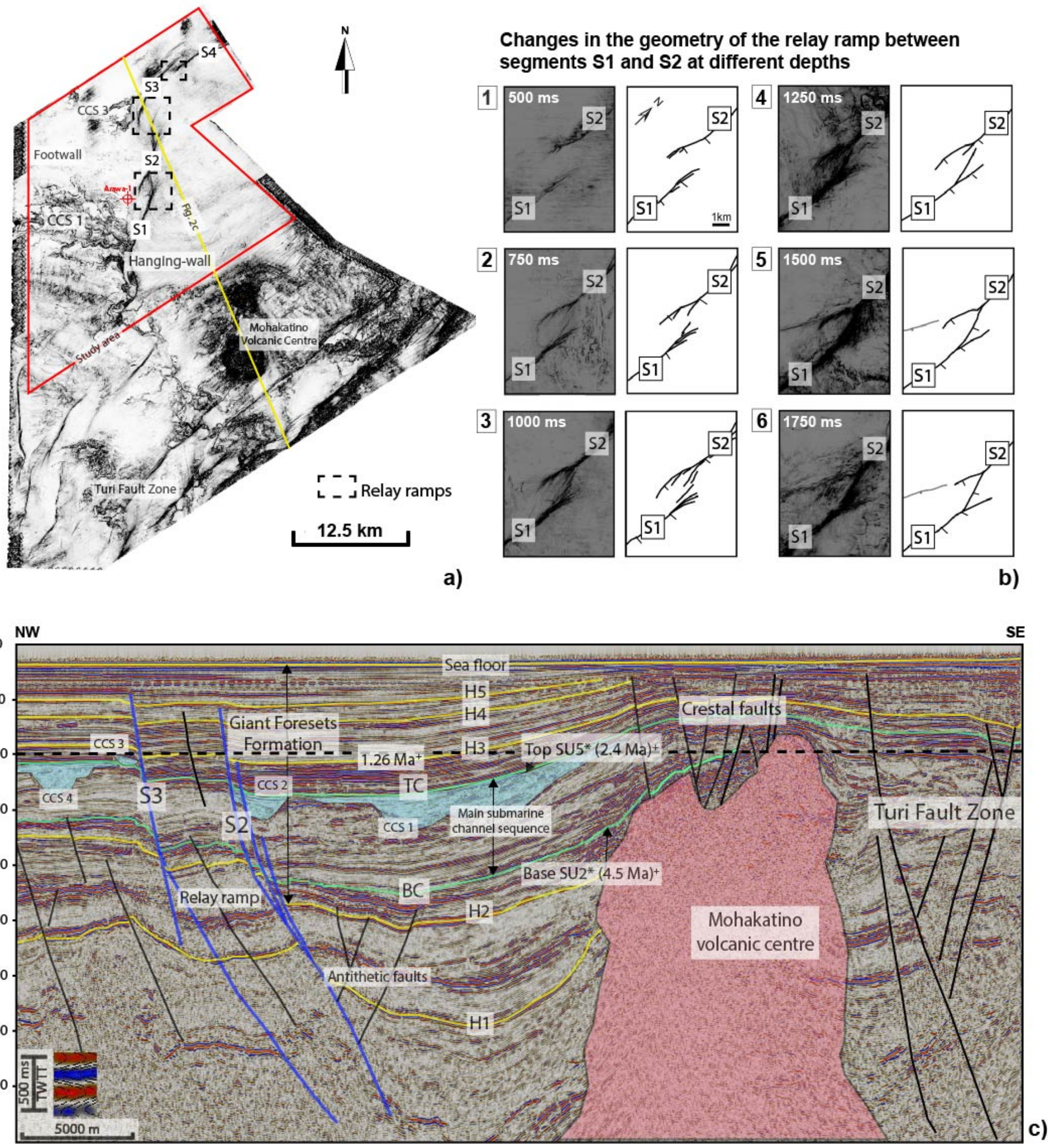

Figure 2: a) Variance slice at -1000 ms TWT showing main structural features in the interpreted seismic volume. The 705 km² study area is delimited by the red polygon. b) Evolution of the relay ramp in the Parihaka Fault at each -250 ms TWT showing the hard linkage of faults with depth. Unbreached relay ramp occur at shallow levels, as shown by the soft linkage of the segments (Modified after Giba et al., 2012). c) Regional seismic profile showing the relay ramp developed between segments S3 and S2 and main channel systems in the study area. The Mohakatino Volcanic Centre is observed to the SE of the seismic line. The main submarine channel sequence is delimited by the horizons traced in green. CCS: channel complex systems. *Correlative seismic units from Salazar et al. (2016). +Correlative ages from Morgans et al. (2006). The location of this profile is indicated in Fig. 2a

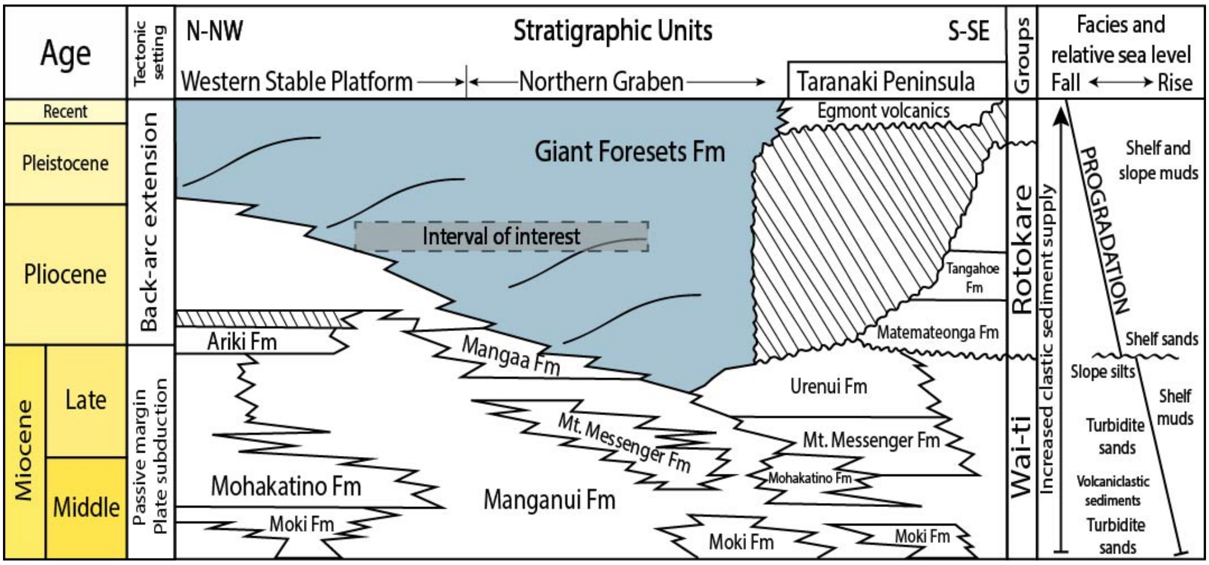

Figure 3: Chronostratigraphic column showing depositional facies and relative sea-level changes in the Taranaki Basin from the Miocene to the Recent. The interval of interest within the Giant Foresets Formation is highlighted in this figure. Modified from King and Thrasher (1996).

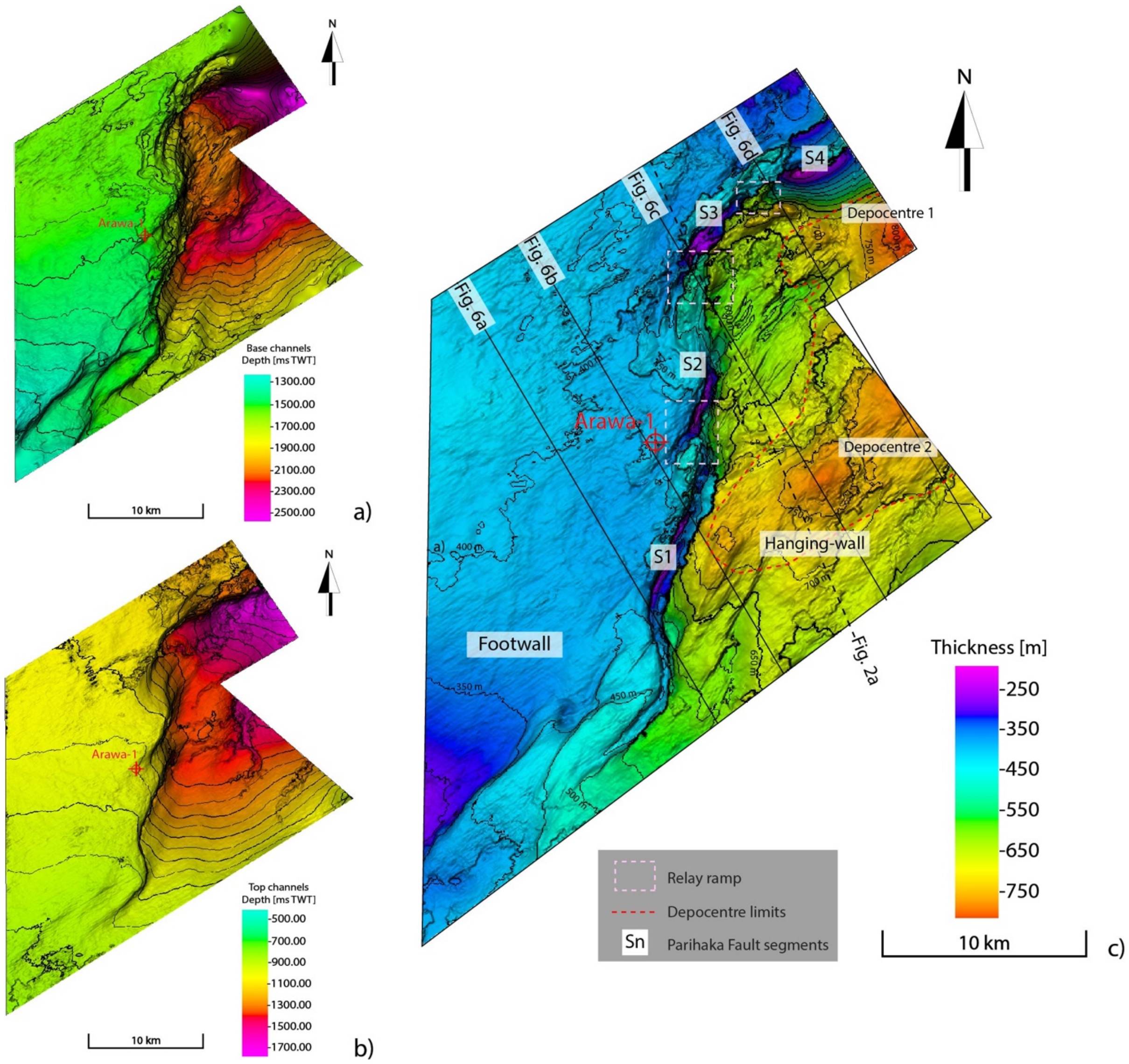

Figure 4: a) Time structure map for the Base Channel (horizon BC), highlighting the great depth in ms TWT difference between the footwall (1250 to 1500 ms TWT) and the hanging-wall blocks (1500 to 2250 ms TWT) of the Parihaka Fault. b) Time structure map for the Top Channel (horizon TC), indicating the depth (in ms TWT) differences between the footwall (900 to 1050 ms TWT) and the hanging-wall (950 to 1450 ms TWT) are smaller than for horizon BC. The interval of the contour lines is 50 ms. c) Isochron map for the between horizons BC and TC. The predominant thickness for the footwall block is 400 m, whereas the thickness for the hanging-wall block ranges from 500 to 800 m. The interval for the contour lines is 50 m. Depocentres 1 and 2 are delimited by the red dashed line and comprise the thickest deposits in the study area.

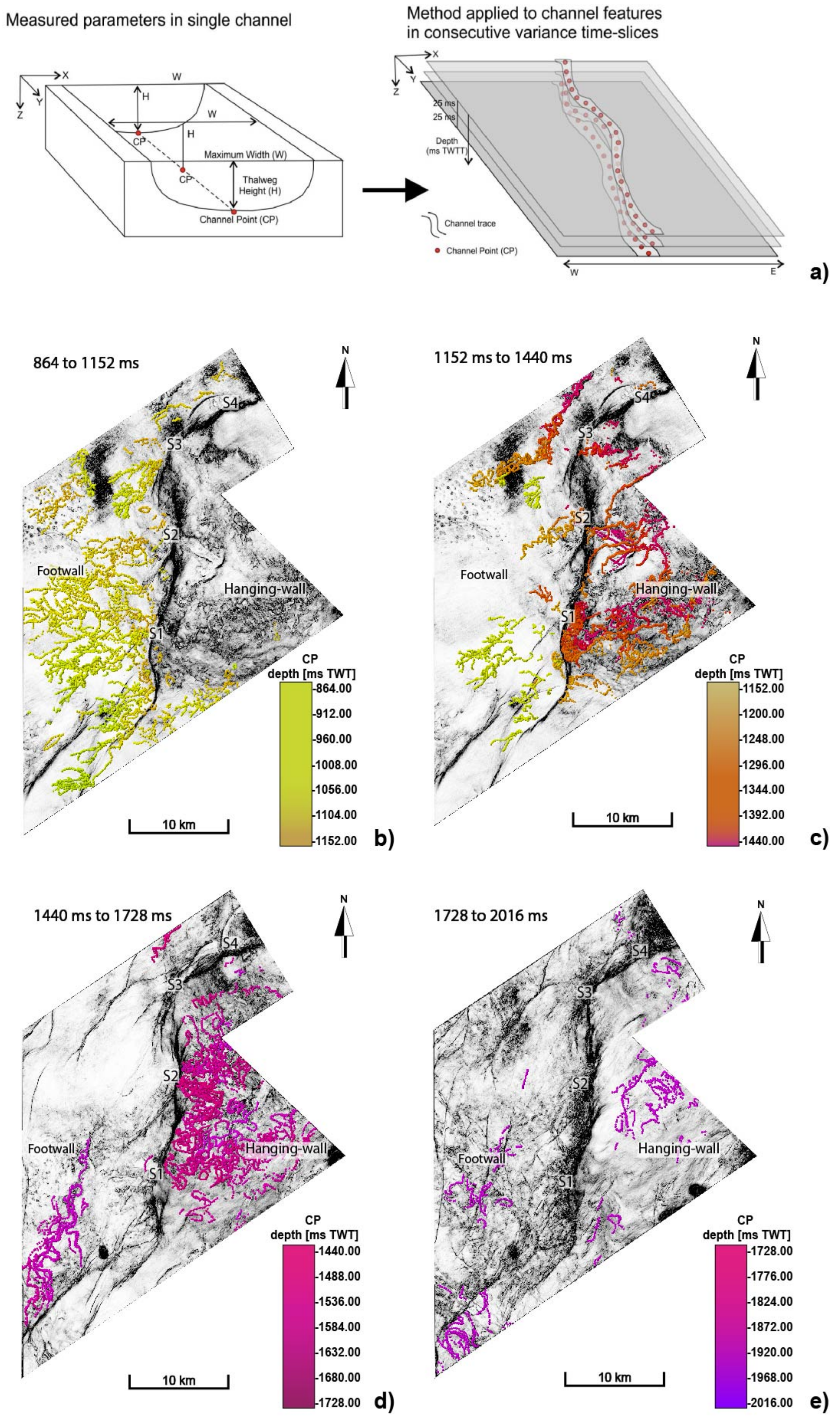
Measured parameters in single channel
Method applied to channel features in consecutive variance time-slices
Maximum Width (W)
Thalweg Height (H)
Channel Point (CP)
Channel trace
Channel Point (CP)
Depth (ms TWTT)
25 ms
25 ms
a)
864 to 1152 ms
1152 ms to 1440 ms
1440 ms to 1728 ms
1728 to 2016 ms
Footwall
Hanging-wall
S1
S2
S3
S4
CP depth [ms TWT]
10 km
b)
c)
d)
e)

632

Figure 5: Schematic representation of the morphometric analysis undertaken in this work. Height and width for channel complex systems were measured from a reference Channel Point (CP) at the base of the variance time-slices. Modified from Gamboa et al. (2012). Channel point distribution maps at depths from b) 864 to 1152 ms TWT, c) 1152 to 1440 ms TWT, d) 1440 to 1728 ms TWT, and e) 1728 to 2016 ms TWT. These maps show channels predominate on the footwall block between 864 and 1152 ms TWT. However, channel complex systems on the footwall block may occur at greater depth. Channels on the hanging-wall block predominate between 1152 to 1728 ms TWT. Channel density is smaller from 1728 to 2016 ms TWT on both in the footwall and hanging-wall blocks of the Parihaka Fault.

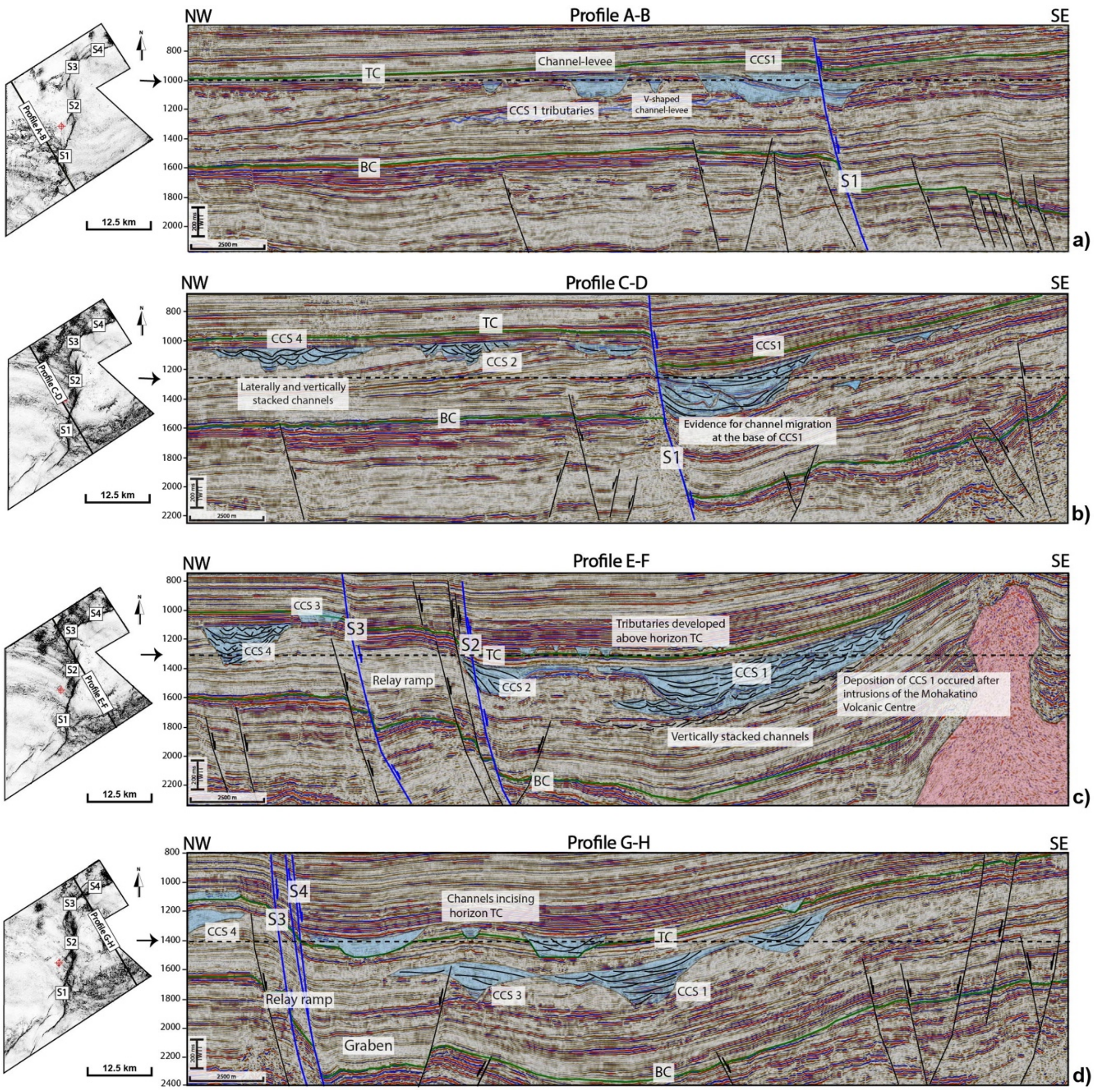

Figure 6: NW-SE seismic profiles of the study area highlighting the relationship between channel complex systems (CCS) and the Parihaka Fault segments. a) Profile A-B shows the tributaries of Channel Complex System 1 to the NW consisting of U and V-shaped erosional bases. Channel Complex System 1 occurs in the SE part of the seismic profile and is offset by segment S1. b) Profile C-D show three of the four main channel systems in the study area. Channel Complex System 4 occurs to the NW on the footwall block and shows laterally and vertically stacked channels. Channel Complex System 2 occurs close to the trace of segment S1 and comprises two tributaries. Channel Complex System 1 occurs entirely on the hanging-wall block in this profile and reveals the lateral and vertical stacking within this channel system. c) Profile E-F shows Channel Complex System 4 system at a greater depth comprising many vertically stacked channels on the footwall block. Channel Complex System 3 also occurs on the footwall block above Horizon TC and close to S3. A rotated relay ramp developed between S3 and S2 is observed. Channel Complex System 2 is offset by S2 at the SE termination of this relay ramp. Channel Complex System 1 occur at observed depths in the seismic survey between 1600 and 1800 ms TWT to the SE. d) Profile G-H shows a relay ramp developed between S3 and S4 in the NE part of the study

area. Channels developed above horizon TC are also observed on the hanging-wall block. The depths of time slices in insets are indicated by an arrow and a dashed line on the seismic profiles.

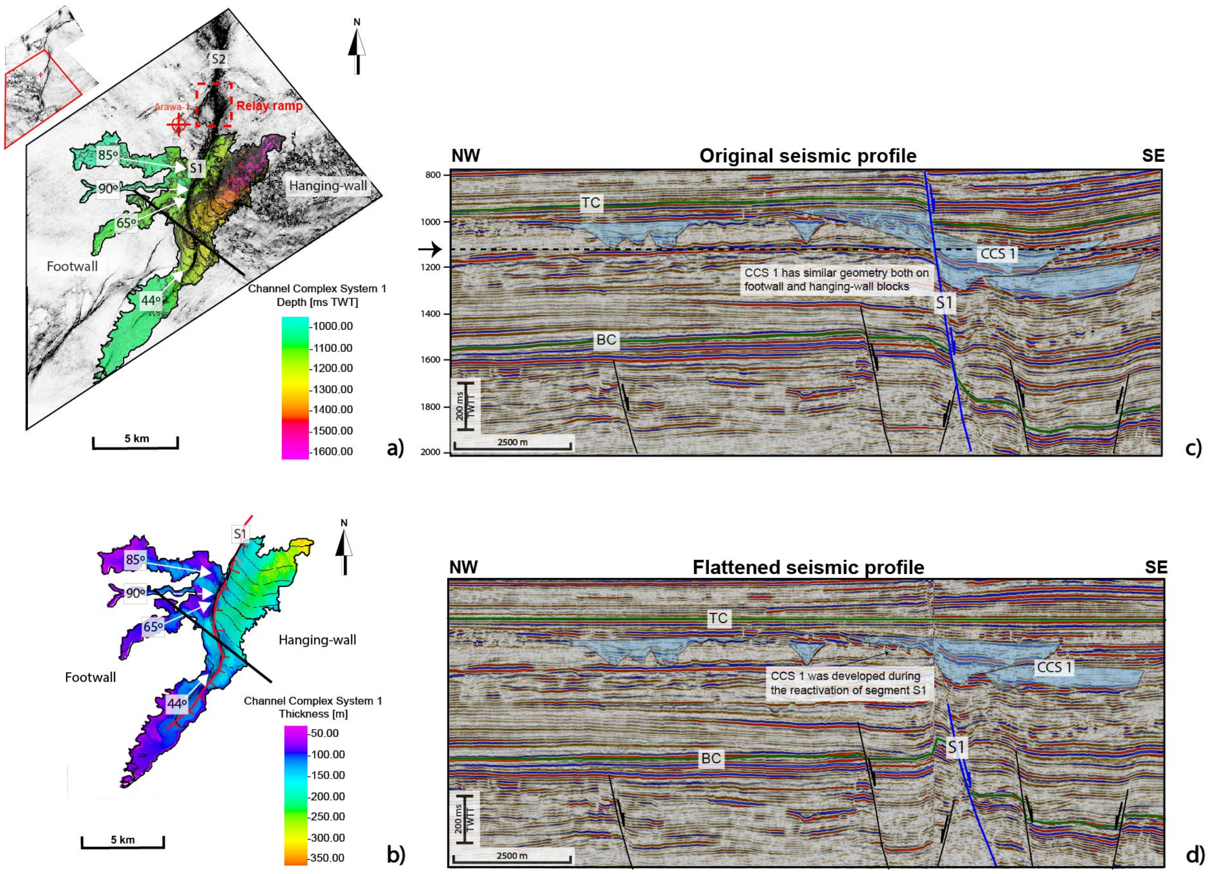

Figure 7: Detailed seismic interpretation of Channel Complex System 1 (CCS 1 in the figure boxes). a) Variance time-slice at 1180 ms showing the base of Channel Complex System 1 on the footwall block, the segments of Parihaka Fault, the position of the seismic section (yellow line), and the angles this channel system make in relation to S1. b) Thickness map for Channel System 1 showing the channel tributaries flowing obliquely to S1. c) Original seismic profile highlighting the channel geometry relative to the Parihaka Fault. The depth of the variance time-slice is indicated by an arrow and a dashed line on the seismic section. d) Seismic profile flattened at horizon TC highlighting the influence of faulting on channel configuration.

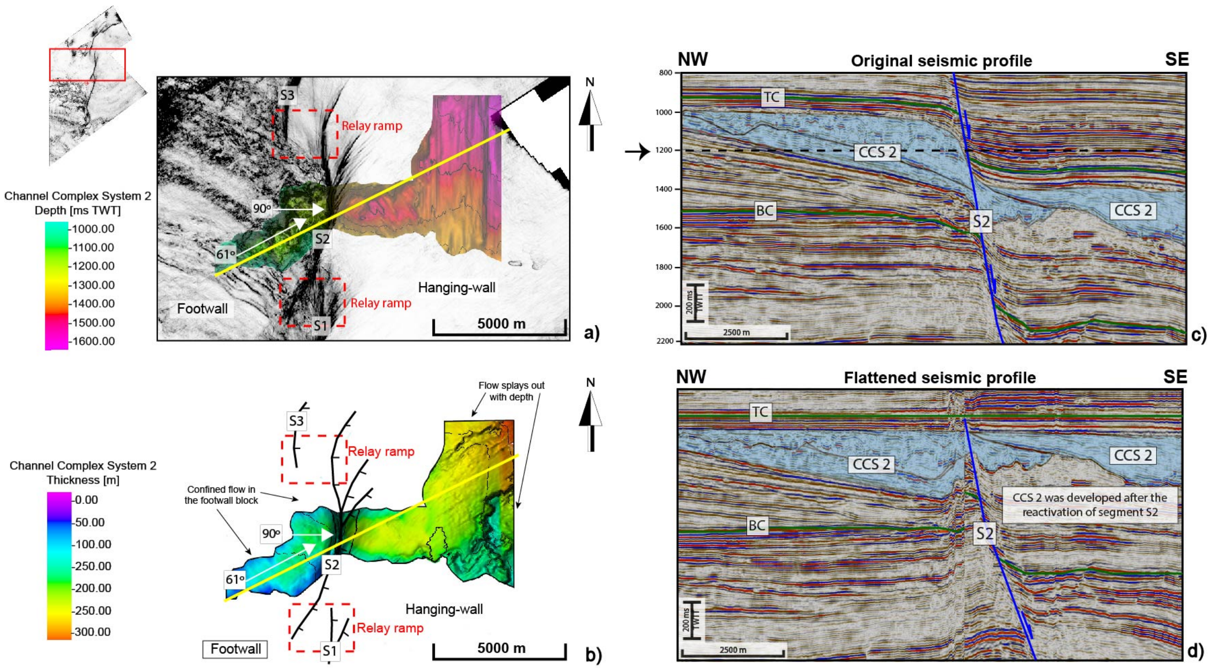

Figure 8: Detailed seismic interpretation of Channel Complex System 2 (CCS 2 in the boxes). a) Variance time-slice at a depth of 1200 ms TWT indicating the base of Channel Complex System 2 on the footwall block, the segments of Parihaka Fault, the position of the seismic section (yellow line), and the angles this channel system make to S2. b) Thickness map for Channel Complex System 2 showing the channel initially flowing obliquely to S2 to later change to a direction transverse to the segment trace. c) Original seismic profile highlighting the channel geometry relative to the Parihaka Fault. The depth of the variance time-slice is indicated by an arrow and a dashed line on the seismic profile. d) Flattened seismic profile at horizon TC showing the syn-tectonic deposition of Channel Complex System 2 during the reactivation of S2.

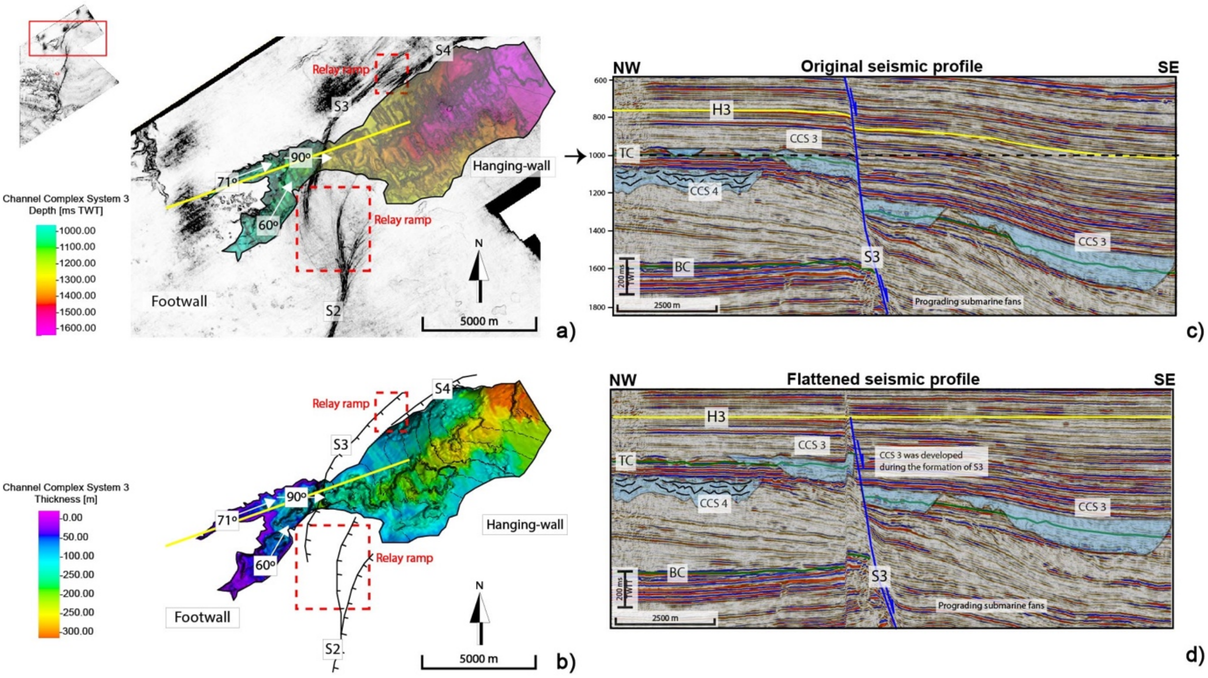

Figure 9: Detailed seismic interpretation of Channel Complex System 3 (CCS 3 in the boxes). a) Variance time-slice at 1020 ms indicating the base of Channel Complex System 3 on the footwall block, the segments of Parihaka Fault, the position of the seismic profile (yellow line), and the angles this channel system make to S3. b) Thickness map for Channel Complex System 3 showing the two main channel tributaries flowing obliquely to segment S3. c) Original seismic profile highlighting the channel geometry relative to the Parihaka Fault. d) Flattened seismic profile at horizon H3 highlighting faulting prior to channel deposition.

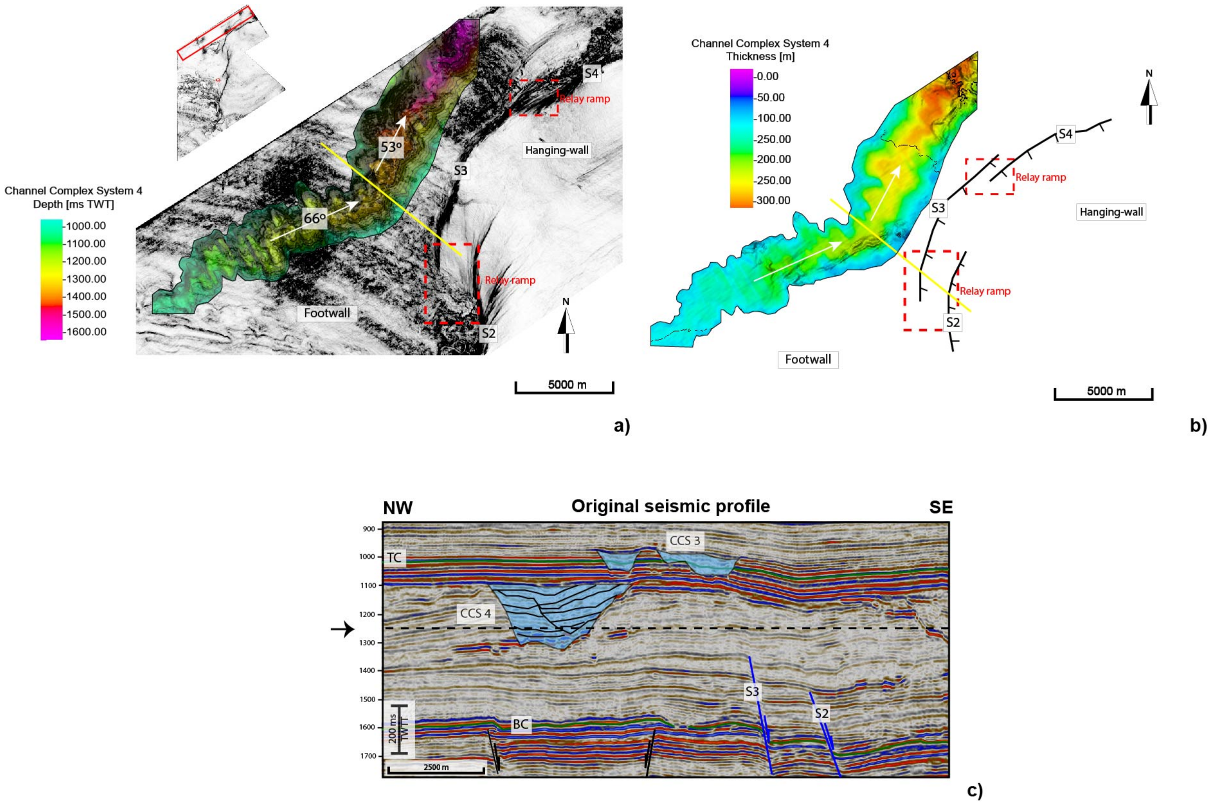

Figure 10: Detailed seismic interpretation of Channel Complex System 4 (CCS 4 in the boxes). a) Variance time-slice at 1320 ms showing the base of Channel Complex System 4 in the footwall block, the segments of Parihaka Fault, the position of the seismic profile (yellow line), and the angles this channel system make to S3. b) Time-structural map for Channel Complex System 4 showing the channel body flowing parallel to the Parihaka Fault trace. c) Selected seismic profile highlighting the channel geometry relative to the Parihaka Fault. Channel Complex System 3 is also observed in this seismic profile above horizon TC.

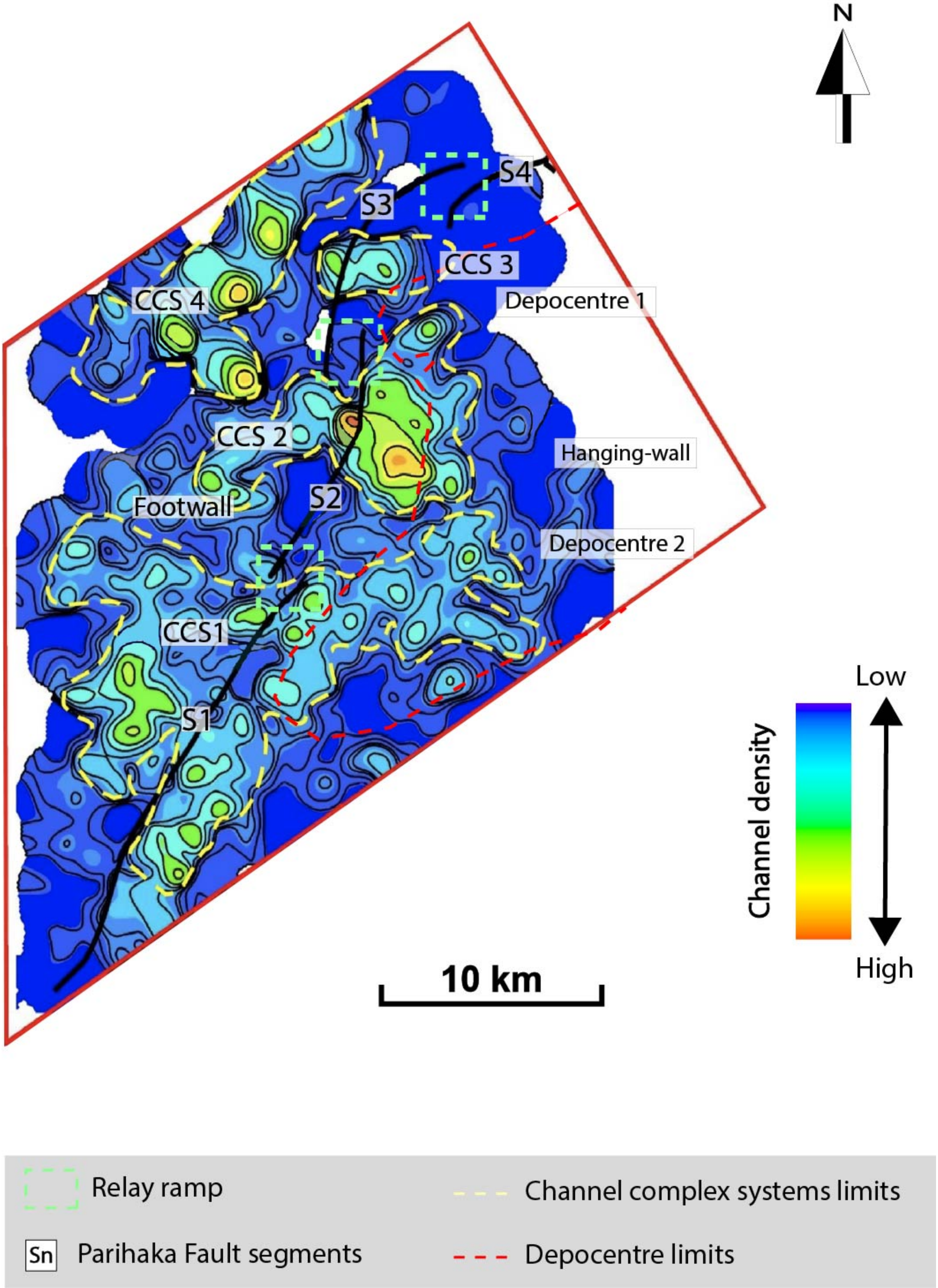

725

726 Figure 11: Channel point density plot showing the lateral and vertical stacking patterns of submarine channel complexes
727 (CCS in the boxes) in the study area. The main channel complex systems were delimited to this plot to facilitate the
728 analysis of the channel density distribution. The greatest channel point density occurs in the areas corresponding to
729 Channel Complex System 4 on the footwall block and Channel Complex System 2 on the hanging-wall block.

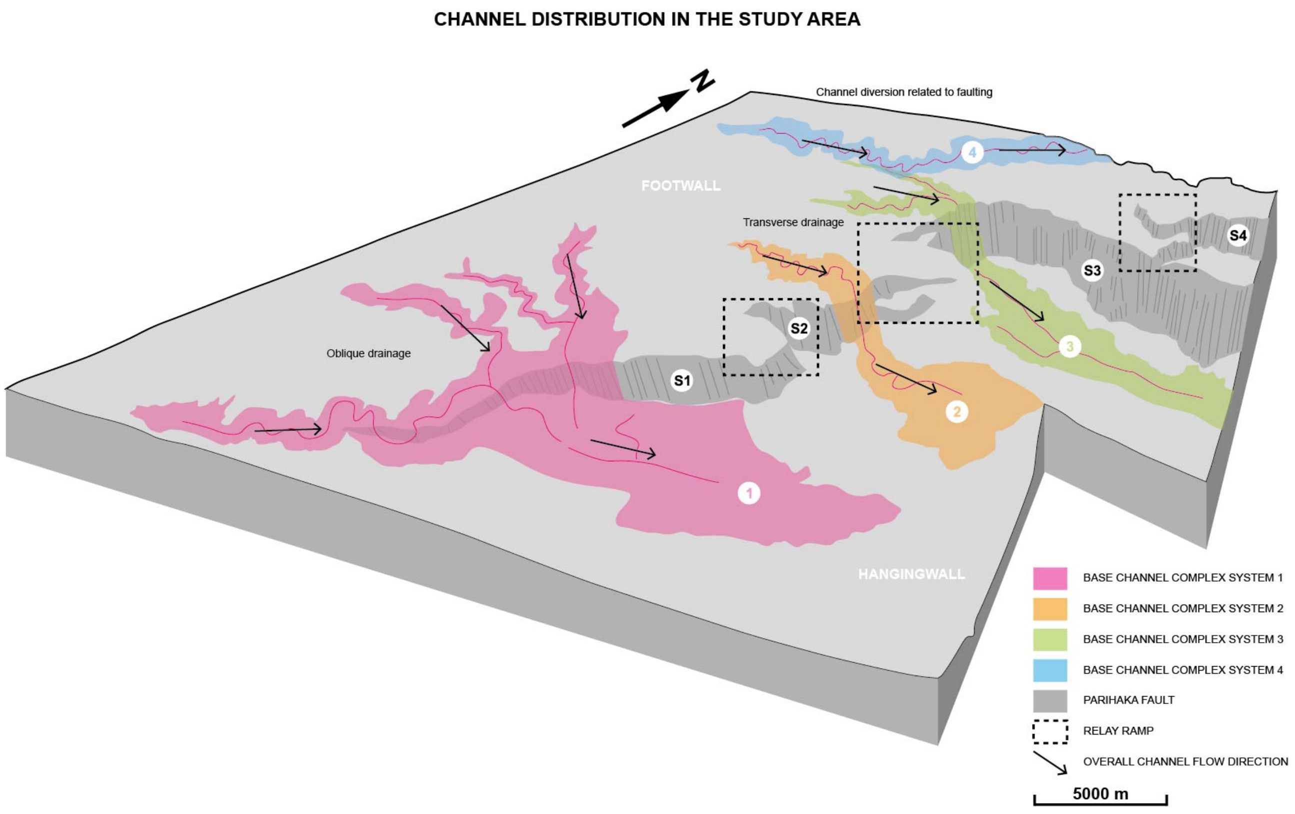

Figure 12: Block diagram summarising the channel distribution the study area indicating the three types of drainage related to the Parihaka Fault trace. In the southern part of the study area, Channel Complex System 1 is an example of oblique drainage, while Channel Complex Systems 2 and 3 in the central parts of the study area are an example of transverse drainage related to a greater displacement of S2 and S3. Channel Complex System 4 is a channel that has changed its course due to the uplift of the footwall block, running parallel to S3.